

## Magnetohydrodynamic Mixed Convection in a Lid-Driven Porous Square Cavity with Internal Elliptic Cold Block and Linearly Heated Side Walls

M. Jahirul Haque Munshi<sup>1,\*</sup>, M. A. Alim<sup>2</sup>, A. H. Bhuiyan<sup>2</sup>

<sup>1</sup>*Department of Mathematics, Hamdard University Bangladesh (HUB), Hamdard Nagar,  
Gazaria, Munshigonj-1510, Bangladesh*

<sup>2</sup>*Department of Mathematics, Bangladesh University of Engineering and Technology  
(BUET), Dhaka- 1000, Bangladesh*

**Abstract:** Magnetohydrodynamic mixed convection in a lid-driven porous square cavity with internal elliptic cold block and linearly heated side walls are numerically simulated in this paper following a finite element method approach. The top moving wall and right wall is cold. The bottom moving wall heated, linearly heated left and right wall, inside the elliptic body are cold. The magnetic field of strength  $B$  is applied parallel to  $x$ -axis. The relevant parameters in the present study are Darcy number ( $Da = 10^{-5} - 10^{-3}$ ), Grashof number ( $Gr = 10^3 - 10^5$ ), Prandtl number  $Pr = 0.7$  and Reynolds number ( $Re = 1 - 10^2$ ). The isotherms are also almost symmetric at small  $Re$  with  $Gr$  ( $Gr = 10^5$ ) and  $Da$  ( $Da = 10^{-3}$ ) and mixed convection is found to be dominant whereas the isotherms are compressed near the left and bottom walls at higher  $Re$  for linearly heated side walls. Results are presented in the form of stream line and isotherms plots as well as the variation of the maximum temperature and Nusselt number at the heat source surface under different conditions. The numerical results indicate the strong influence of the mentioned parameters on the flow structure and heat transfer as well as average Nusselt number. An optimum combination of the governing parameters would result in higher heat transfer.

**Keywords:** *Mixed convection; Square cavity; Elliptic obstacle; Lid-driven cavity; FEM*

**Introduction:** Mixed convection is a combination of both natural and forced convection. Mixed convection square cavities with inner obstacle have been well studied over a century. Also mixed convection is a very promising phenomenon now days and associated with a wide range of industrial applications. Applications of lid-driven conveyer belt, Escalator and lift of elevator, ventilation, heating and cooling flows in buildings, heat transfer for electronics packaging applications. In future, lid-driven square cavity of mixed convection related problems will be more challenging.

Heat transfer and fluid flow in porous media filled enclosures or channels have important engineering applications such as filtration, separation processes in chemical industries, solar collectors, heat exchangers, etc. Studies on thermal convection in porous media and state-of-the-art reviews are given by Bejan [1]. The literature detailed concerning the porous media in the books by J. N. Ready [2], O. S. Zienkiewicz et al. [3], T. K. Bask et al. [4], M. Sathiyamoorthy [5].

---

**Article history:**

Received 20 April 2017

Received in revised form 10 May 2017

Accepted 10 June, 2017

Available online 30 June 2017

---

**Corresponding author details:**

E-mail : [jahir.buet.bd@gmail.com](mailto:jahir.buet.bd@gmail.com)

Tel: +8801819274767

Copyright © 2017 BAUET, all rights reserved

The modern technologies require through understanding of the pertinent processes involved in these fields. Considerable research work has been reported in the literature on natural convection due to combined thermal and mass buoyancy forces. Unfortunately, pure natural or pure forced convection situations seldom arise in practice. The involvement of both natural and forced convection, referred as mixed convection, in porous media has been an important topic because of its wide range of application in engineering and science. The governing non-dimensional parameter for the description of flows are Grashof number ( $Gr$ ), Reynolds number ( $Re$ ), Prandtl number ( $Pr$ ) and Darcy number ( $Da$ ). Another important non-dimensional parameter, Richardson number characterizes mixed convection flow where  $Gr$  and  $Re$  represent the strength of the natural and forced convection flow effect, respectively. The detailed literature concerning convective flow in porous media is available in the books by Nield and Bejan [6]. Oztop [7] investigated numerically combined convection heat transfer and fluid flow in a partially heated porous lid-driven cavity. Volume averaged equations governing unsteady, laminar, mixed convection flow in an enclosure filled with a Darcian fluid-saturated uniform porous medium in the presence of internal heat generation is investigated by Khanafer and Chamkha [8]. Chamkha [9] also studied the mixed convection flow along a vertical permeable plate embedded in a porous medium in the presence of transverse magnetic field and non-Darcy fully developed steady laminar mixed convection flow of an electrically conducting and heat generation/absorption fluid in a porous medium channel. Mixed convection in porous cavity has also been analyzed in presence of internal heat generation. Khanafer and Chamka [10] analyzed laminar, mixed convection flow in a Darcian fluid-saturated porous cavity in the presence of internal heat generation and they found that the flow and the heat transfer inside the cavity were strong function of Richardson number ( $Ri$ ). A recent investigation of Bask et al. [11] was based on mixed convection of fluid within a cavity in presence of uniform and non-uniform bottom heating while the top plate is maintained at uniform velocity. This work [12] analyzed flow and temperature characteristic as functions of Prandtl number ( $Pr$ ) and Rayleigh number ( $Ra$ ) and the heat transfer rates have been estimated via local and average Nusselt numbers as a function of  $Ra$  for various model fluid or  $Pr$ . Khanafer et al. [13] and Al-Amiri et al. [14] studied numerically mixed convection in a lid-driven cavity filled with a porous medium. M. Jahirul Haque Munshi et al. [15, 16] numerically investigated effects on mixed convection in a square cavity with inside elliptic shape block. On the basis of the literature review, it appears that very little work was reported on the Magneto hydrodynamic mixed convection in a lid-driven porous square cavity with internal elliptic cold block and linearly heated side walls. Thus, the obtained numerical results of the present problem are presented graphically in terms of streamlines, isotherms, temperature, velocity, local Nusselt number for different Darcy numbers, Grashof numbers and Reynolds numbers.

**Problem Formulations:** Two-dimensional square cavity is illustrated in Figure 1. The width and height of the cavity are denoted as  $L$ . The heated wall denoted by  $T_h$  and cold wall denoted by  $T_c$  respectively. The arrangement of the moving and linearly heated has great impact on the fluid flow structures in the enclosure as follows:

**Case I.** The left wall linearly heated, upper and right wall cold, lower wall heated and inside elliptic obstacle cold, upper and lower wall moving.

**Case II.** The left and right wall linearly heated, upper wall cold, lower wall heated and inside elliptic obstacle cold, upper and lower wall moving.

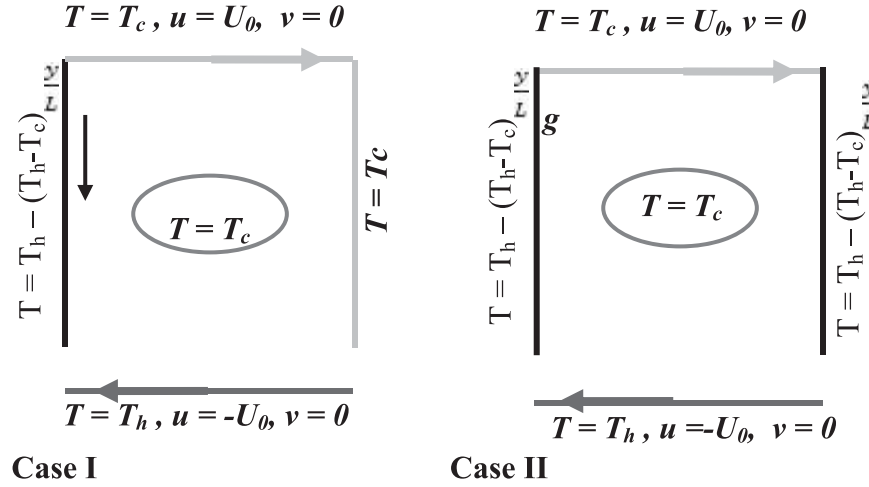


**Fig. 1:** Schematic diagram of the physical system

**Governing Equations:** The governing equations for steady two-dimensional mixed convection flow in a lid-driven porous square cavity using conservation of mass, momentum and energy can be written with the following dimensionless variables T. Basak et al. [12]

$$\frac{\partial U}{\partial X} + \frac{\partial V}{\partial Y} = 0, \quad \text{eq. 1}$$

$$U \frac{\partial U}{\partial X} + V \frac{\partial U}{\partial Y} = -\frac{\partial P}{\partial X} + \frac{1}{Re} \left( \frac{\partial^2 U}{\partial X^2} + \frac{\partial^2 U}{\partial Y^2} \right) - \frac{1}{Re Da} U, \quad \text{eq. 2}$$

$$U \frac{\partial V}{\partial X} + V \frac{\partial V}{\partial Y} = -\frac{\partial P}{\partial Y} + \frac{1}{Re} \left( \frac{\partial^2 V}{\partial X^2} + \frac{\partial^2 V}{\partial Y^2} \right) - \frac{1}{Re Da} V + \frac{Gr}{Re^2} \theta, \quad \text{eq. 3}$$

$$U \frac{\partial \theta}{\partial X} + V \frac{\partial \theta}{\partial Y} = \frac{1}{Re Pr} \left( \frac{\partial^2 \theta}{\partial X^2} + \frac{\partial^2 \theta}{\partial Y^2} \right). \quad \text{eq. 4}$$

**The transformed boundary conditions are:** At the cold top walls:  $\theta = 0, U = 1, V = 0$

At the heated bottom wall:  $\theta = 1, U = -1, V = 0$

Linearly heated left wall:  $\theta = 1 - Y, U = 0, V = 0$

Linearly heated right wall:  $\theta = 1 - Y$  or  $0$ , and  $U = 0, V = 0$

At the cold elliptic body:  $U = 0, V = 0, \theta = 0$ .

The following dimensionless variables and parameters have been used in Eqs. (1)-(4):

$$X = \frac{x}{L}, \quad Y = \frac{y}{L}, \quad U = \frac{u}{U_0}, \quad V = \frac{v}{U_0}, \quad \theta = \frac{T - T_c}{T_h - T_c}$$

$$P = \frac{p}{\rho U_0^2}, \quad Pr = \frac{\nu}{\alpha}, \quad Da = \frac{K}{L^2}, \quad Re = \frac{U_0 L}{\nu}, \quad Gr = \frac{g \beta (T_h - T_c) L}{\nu^2} \quad \text{eq. 5}$$

Note that, thermal diffusivity ( $\alpha$ ) and kinematic viscosity ( $\nu$ ) in Eq. (4) are defined based on local thermal equilibrium between solid and fluid within a porous control volume D. A. Nield et al. [6] where  $\alpha = \frac{k_{eff}}{\phi \rho_0 c_{pf}}$  and  $\nu = \frac{\mu_f}{\rho_0}$ . Here  $k_{eff}$  is the effective thermal conductivity of the porous matrix,  $\phi$  is the porosity,  $c_{pf}$  is the specific heat of fluid,  $\mu_f$  is the viscosity of fluid and  $\rho_0 = \rho$  is the density of fluid at  $\theta = 0$ .

**Grid Refinement Test:** A grid independence test is reported with  $Pr = 0.7$ ,  $Re = 100$ ,  $Da = 10^{-3}$  and  $Gr = 10^5$  in order to decide the suitable grid size for the study. The extreme values of the mean Nusselt number ( $Nu$ ) that relates to the heat transfer rate of the heated surface and the average temperature ( $\theta_{av}$ ) of the fluid in the square cavity are used as sensitivity measures of the correctness of the solution.

**Table 1.** The addition of the quantities  $Nu$  and  $\theta_{av}$  on the grid size are shown in Table

Nodes (elements)	8945 (15297)	3517 (6790)	1785 (3358)	658 (1212)	576 (1043)	493 (957)
$Nu$	352098	3.52062	3.51875	3.51245	3.51045	3.50118
$\theta_{av}$	0.54487	0.54298	0.54185	0.54027	0.53981	0.53855

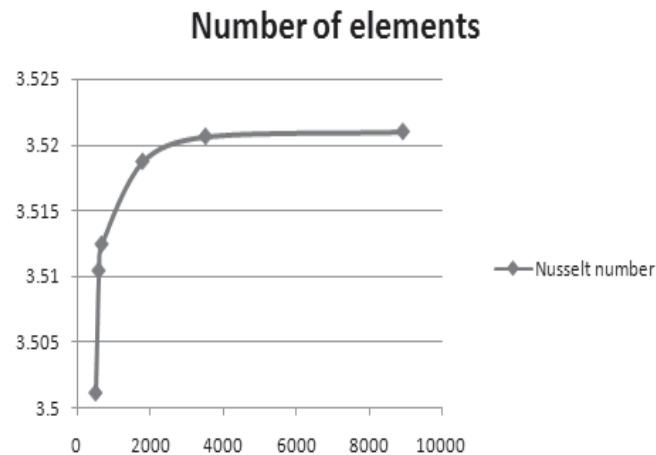


**Fig. 2:** Effect of grid refinement test on average Nusselt number

**Mesh Generations:** In finite element method, the mesh generation is the technique to subdivide a domain into a set of sub-domains, called finite elements, control volume etc. The discrete locations are defined by the numerical grid, at which the variables are to be calculated. The computational domains with irregular geometries by a collection of finite elements make the method a valuable practical tool for the solution of boundary value problems arising the various fields of engineering. Fig. 3 displays the finite element mesh of the present physical domain.

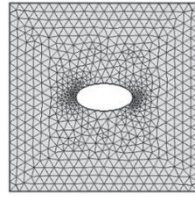


**Fig. 3:** Mesh generation of mixed convection in square cavity

**Numerical Techniques:** This paper represents new numerical results better than the problem Analysis of mixed convection in a lid-driven porous square cavity with linearly heated side wall(s) by T. Basak et al. [12]. Streamlines and isotherms are plotted in Fig. 4: showing good agreement.

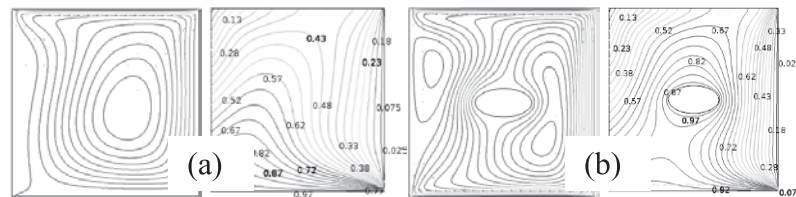


**Fig. 4:** Streamline and isotherms for different Grashof number Present study (a) without obstacle (b) with elliptic obstacle

Nusselt number Table						
Gr	Without obstacle		With obstacle		% increase in heat transfer	
	Re = 100	Re = 1	Re = 100	Re = 1	Re = 100	Re = 1
1000	3.0133	2.9969	3.84999	3.86637	27	29
10000	2.99448	3.77787	3.85849	4.8715	28	28
100000	3.35433	8.11676	4.53785	9.41524	35	16

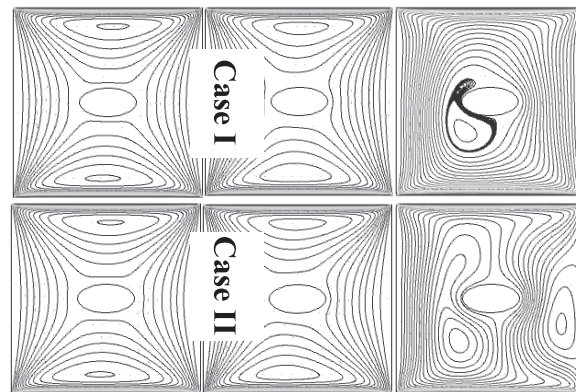
**Results and Discussion:** In this section, results of the numerical study has been performed to simulate the optimization of mixed convection in a lid-driven porous square cavity with internal elliptic shape cold block and linearly heated side wall. With this aim, results will be presented via streamlines, isotherm, Nusselt number, and temperature and velocity profiles in next parts of the work.

**Effect of Grashof number:** Fig. 5 and 6 illustrate the streamlines and isotherms involving uniformly heated bottom wall, linearly heated left wall and cooled right wall for  $Gr = 10^3$  to  $10^5$ ,  $Pr = 0.7$ ,  $Da = 10^{-3}$  at  $Re = 100$ , respectively. For  $Pr = 0.7$  and  $Re = 100$ , the strength of the buoyancy inside the cavity is significant and more fluid rise from the upper and lower cavity at  $Gr = 10^3$  and  $10^4$ . As  $Gr$  increases to  $10^5$ , the strength of the buoyancy increases and elliptic shape eyes inside the cavity. As can be seen from the streamlines in the Fig. 5 (Case II), a pair of counter-rotating eddies are formed in the left and right half of the cavity for all Grashof numbers,

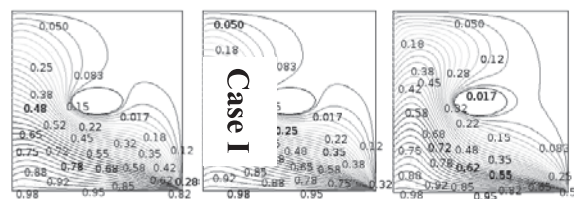


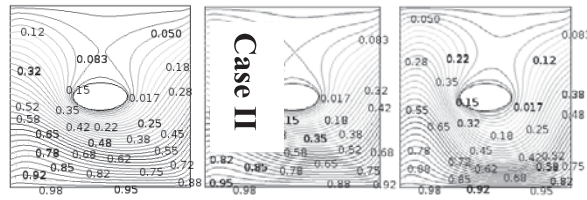
Darcy number and Reynolds number considered. Comment to both cases, the heat transfer is due to conduction as the strength of circulation is lower. At  $Gr = 10^5$ , the mixed convection becomes dominant as the lid-driven flow and the strength of both the circulations are increased. Due to uniform heating of the bottom wall and linearly heated side walls, fluid rise from the of side walls the cavity forming two almost symmetric rolls with clockwise rotations inside the cavity. Conduction dominant heat transfer is observed from the isotherms in Fig. 6. It can be seen from the isotherms line bending lower left corner of the square cavity. Also the isotherms for same parameters with Fig. 6 (Case II) the isotherms line more bending lower and side walls positions. As a result isotherms lines are developed.

Fig. 7 are plotted to see the variation of local Nusselt number, velocity, and temperature different values of Grashof number. For Case I, local Nusselt number various x direction becomes lower for higher values of Grashof number and y direction becomes maximum and minimum line in the cavity. Again the velocity starts at maximum point of the left wall and moves to the right wall at minimum points. For Case II, It can be seen from the Figure that the maximum and minimum value of local Nusselt number increasing with increasing the Grashof number and also present the velocity start at maximum points and decreasing the bottom wall for different Grashof number.



**Fig. 5:** Illustrate the streamlines involving heated bottom moving wall, linearly heated left and right wall, upper cold moving wall and elliptic shape cold with  $Pr = 0.7$ ,  $Re = 100$  and  $Da = 10^{-3}$  for  $Gr = 10^3$  to  $10^5$





**Fig. 6:** Illustrate the isotherms involving heated bottom moving wall, linearly heated left and right wall, upper cold moving wall and elliptic shape cold with  $Pr = 0.7$ ,  $Re = 100$  and  $Da = 10^{-3}$  for  $Gr = 10^3$  to  $10^5$

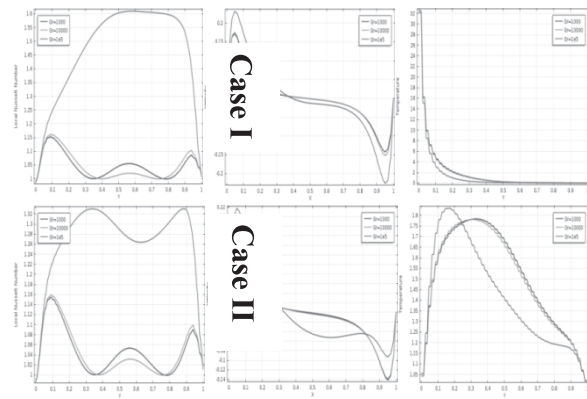


**Fig. 7:** Variation of Local Nusselt number, Velocity and Temperature of the square cavity with Grashof number  $Gr = 10^3$  to  $10^5$

**Effect of Darcy number:** Fig. 8 and Fig. 9 illustrate the streamlines and isotherms inside the cavity with the effect of Darcy and prandtl numbers respectively. As can be observed from the figures with existence of the symmetrical boundary conditions about the side walls, the flow and temperature fields are symmetrical about this line. As can be seen from the streamlines in the Fig. 8, a pair of counter- rotating elliptic shape eyes is formed in the left upper corner and right middle of the cavity for all Darcy numbers considered. Each cell ascends through the symmetry axis, this phenomenon means increasing Darcy number in the flow velocity increasing. Conduction dominant heat transfer is observed from the isotherms in Fig. 9, at Darcy and prandtl numbers. As can be seen from the isotherms line bending the left and right wall respectively. When Darcy number increasing isotherms condense left and right wall which means increasing heat transfer through convection. Finally from the isotherms, it can observe that with increase in Darcy number, mixed convection is suppressed and heat transfer occurs mainly through conduction. Fig. 9 shows the effect of Darcy number for  $Pr = 0.015$ ,  $Re = 100$  and  $Gr = 10^5$ . The primary circulation occupies most of the cavity, however, the strength of circulation is weak at  $Da = 10^{-5}$ . As the Darcy number increasing to  $10^{-4}$ . Further increase of Darcy number to  $10^{-3}$  show that the strength of primary and secondary circulations increases and the maximum value of streamlines. All the isotherms are smooth symmetric curves that span the entire cavity. Thus at  $Re = 100$ , the conduction dominant mode of heat transfer prevails for  $Da = 10^{-5}$  to  $10^{-3}$ .

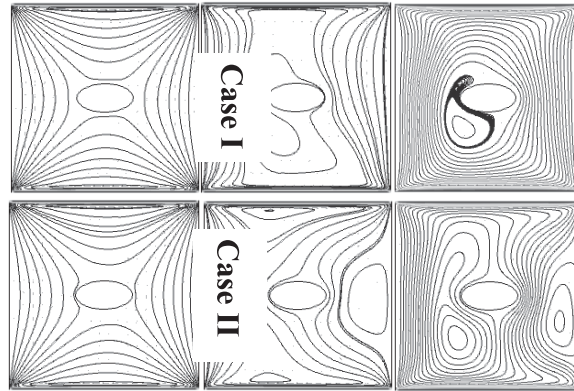


**Fig. 8:** Streamlines and isotherms for linearly heated left walls and cold right wall with  $Pr = 0.7$ ,  $Re = 100$  and  $Gr = 10^5$  for: (a)  $Da = 10^{-5}$ ; (b)  $Da = 10^{-4}$ ; (c)  $Da = 10^{-3}$

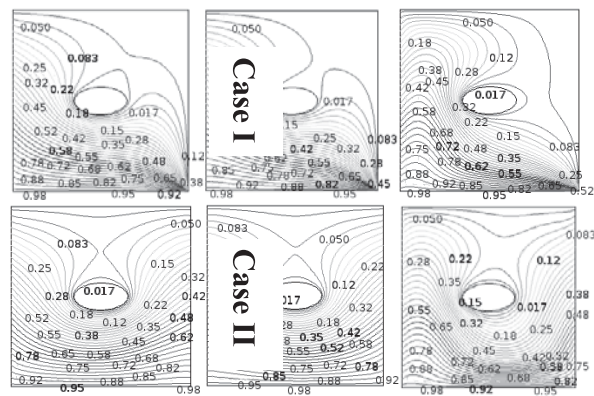


**Fig. 9:** Isotherms for linearly heated left wall and cold right wall with  $Pr = 0.7$ ,  $Re = 100$  and  $Gr = 10^5$  for: (a)  $Da = 10^{-5}$ ; (b)  $Da = 10^{-4}$ ; (c)  $Da = 10^{-3}$

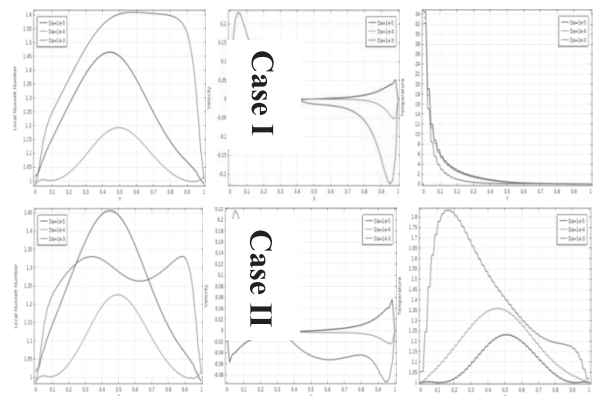


**Fig. 10:** Variation of temperature gradient along the right wall of the square cavity with Darcy number

Variations of the local Nusselt number along the hot bottom wall with x- axis the Darcy numbers are shown in Fig. 10. It can be seen from the figure that the local Nusselt number increases with



the Darcy number in major portion of the hot wall (Case I). Also as can be observed (Case II) from the figure in whole portion of the cavity the local Nusselt number decreases with increases in the Darcy numbers. Also shows the velocity profile along the vertical direction at the mid axis in y-direction at different Darcy numbers. Fig. 10 (Case I) presents that the velocity magnitude increases with an increases of Darcy numbers. In similar manner, Fig. 10 (Case II) shows that the velocity profile increases with an increase of Darcy numbers. Maximum and minimum points are observed due to flows. Variation of the temperature of the absolute value of maximum and minimum value of temperature increases with the decrease of the Darcy number.

**Effect of Reynolds number:** Fig. 11 displays the effect of Reynolds numbers on the flow fields in the cavity operating at three different values of  $Re$  ( $= 1, 10, 100$ ), with  $Pr = 0.7$ ,  $Gr = 10^5$  and  $Da = 10^{-3}$ . It is observed that natural convection is dominant at low value of  $Re$  with  $Pr = 0.7$  and elliptic shape eyes are formed in the cavity as shown in figure. As  $Re$  increases to 10, due to increase of inertia effect, the forced convection gradually becomes dominant over natural convection.

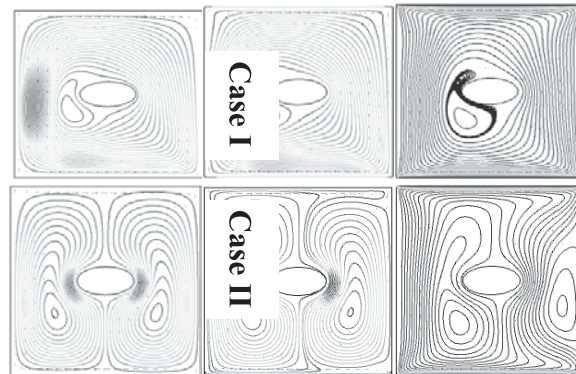


**Fig. 11:** Streamlines and isotherms for linearly heated left wall and cold right wall with  $Pr = 0.7$ ,  $Gr = 10^4$  and  $Da = 10^{-3}$  for: (a)  $Re = 1$ ; (b)  $Re = 10$ ; and (c)  $Re = 100$

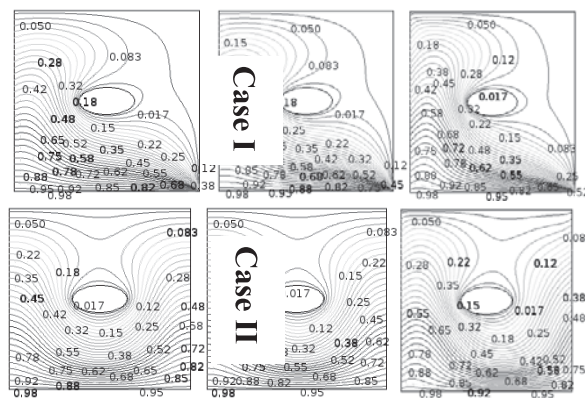


**Fig 12:** Isotherms for linearly heated left wall and cold right wall with  $Pr = 0.7$ ,  $Gr = 10^4$  and  $Da = 10^{-3}$  for: (a)  $Re = 1$ ; (b)  $Re = 10$ ; and (c)  $Re = 100$

The right circulation cells are gradually deformed due to motion of upper lid and left circulation cell still denotes the dominant effect of natural convection. As  $Re$  increases to  $10^2$ , the secondary circulation almost disappears and primary circulation occupies most of the cavity due to enhanced forced convection. The isotherms are also found to be non-symmetric showing forced convection dominant heat transfer.

As  $Pr$  increases to 10, for low value of  $Re = 1$ , the secondary circulation cells appear near the bottom wall. Both primary and secondary circulation cells are found to be symmetric for  $Re = 1$ . As  $Re$  increases to 10, the forced convection gradually becomes dominant over natural convection, hence the strength of secondary circulation cell reduces and right cell starts to deform due to the motion of the top wall. The isotherms also tend to compress towards left showing convection dominant effect. The dominance of forced convection leads to greater degree of thermal mixing near the upper portion of right half of the cavity. As  $Re$  increases to  $10^2$ , the primary circulation cell gets deformed towards the middle portion of the left wall and the secondary circulation cell near the bottom portion of the right wall tends to grow.

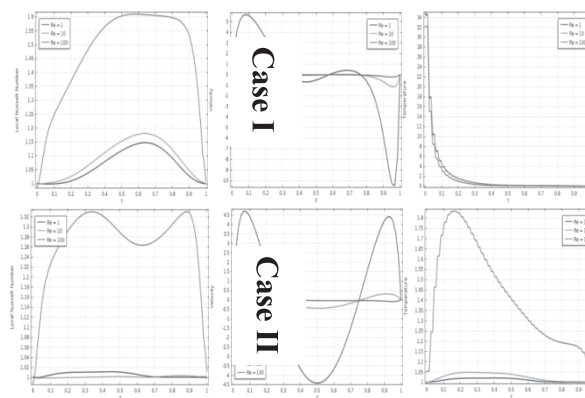


**Fig. 13:** Variation of temperature gradient along the right wall of the square cavity with Reynolds number.

**Conclusions:** The current investigation addresses two-dimensional laminar mixed convection in a lid-driven square cavity filled with porous medium with internal elliptic block and the variation of heat generation parameters in the present study are Darcy number ( $Da = 10^{-5} - 10^{-3}$ ) Grashof number ( $Gr = 10^3 - 10^5$ ), Prandtl number ( $Pr = 0.015-10$ ) and Reynolds number ( $Re = 1-10^2$ ). The effect of varying the mentioned parameters on the distribution of streamlines, isotherms, average Nusselt number at the hot wall. The following are concluded from the obtained results: A heat generation parameter has a significant effect on streamlines during the mixed convection dominated regions. At the same time, it has a significant effect on thermal fields at the three convection regimes. The isotherms are in general symmetric at smaller  $Pr$  irrespective of  $Da$  and  $Re$  at  $Gr = 10^5$  for linearly heated left wall and cold right wall. Interesting results are obtained at higher  $Pr$ ,  $Gr$  and  $Da$  with various regimes of  $Re$ . the isotherms are almost symmetric at small

$Re$  with higher  $Gr$  ( $Gr = 10^5$ ) and  $Da = 10^{-3}$  and natural convection is found to be dominant whereas, forced convection leads to compressed isotherms near the left and bottom walls at higher  $Re$  for linearly heated side walls.

### Acknowledgements:

The authors wish to acknowledge Department of Mathematics, Faculty of Science, Engineering and Technology, Hamdard University Bangladesh (HUB), Gazaria, Munshiganj-1510, Bangladesh, for support and technical help throughout this work.

### References:

- [1] A. Bejan, I. Dincer, S. Lorente, A.F. Miguel, A.H. Reis, Porous and Complex Flow Structures in Modern Technologies, Springer, New York, 2004.
- [2] J.N. Reddy, An Introduction to Finite Element Analysis, McGraw-Hill. New York, 1993.
- [3] O.C. Zienkiewicz, R.L. Taylor, J.M. Too, Reduced integration technique in general analysis of plates and shells, Int. J. Numer. Meth. Eng., vol. 3(1971), pp. 275- 290.
- [4] T. Basak, S. Roy, T. Paul, I. Pop, Numerical convection in a square cavity filled with a porous medium: effects of various thermal boundary conditions, Int. J. Heat Mass Transfer, vol. 49(2006), pp. 1430- 1441.
- [5] M. Sathiyamoorthy, T. Bask, S. Roy, I. Pop, Steady natural convection flow in a square cavity filled with a porous medium for linearly heated side wall (s), Int. J. Heat Mass Transfer 50(2007), pp. 1892- 1901.
- [6] D.A. Nield, A. Bejan, Convection in Porous Media, third ed., Springer, Berlin
- Ingham, D. B., Pop, I. (eds.), Transport phenomena in porous media, Pergamon, Oxford, UK, 1998
- [7] Oztop, H. F., Combined convection heat transfer in a porous lid-driven enclosure due to heater with finite length, Int. Commun. Heat Mass Transfer 33(2006), pp. 772-779.
- [8] A.J. Chamka, A.R.A. Khaled, Nonsimilar hydromagnetic simultaneous heat and mass transfer by mixed convection from a vertical plate embedded in a uniform porous medium, Numer. Heat Transfer A 36(1999), pp. 327- 344.
- [9] A.J. Chamka, Mixed convection flow along a vertical permeable plate embedded in a porous medium in the presence of a transverse magnetic field, Numer. Heat Transfer A 34 (1998), pp. 93- 103.
- [10] Khanafer, K. M., Chamka, A. J., Mixed convection flow in a lid-driven enclosure filled with a fluid-saturated porous medium, Int. J. Heat Mass Transfer 42(1999), pp. 2465-2481.
- [11] T. Basak, S. Roy, P.K. Sharma, I. Pop, Analysis of mixed convection flows within a square cavity with uniform and non-uniform heating of bottom wall, Int.J. Therm. Sci. 48(2009), pp. 891- 912.
- [12] T. Basak, S. Roy, S. K. Singh, I. Pop, Analysis of mixed convection in a lid-driven porous square cavity with linearly heated side walls, Int. J. Heat Mass Transfer 53 (2010), pp. 1819-1840.
- [13] Khanafer, K., Vafai, K., Double-diffusive mixed convection in a lid-driven enclosure filled with a fluid-saturated porous medium, Numer. Heat Transfer A, vol. 42(2002), pp. 465-486.
- [14] Al-Amiri, A. M., Analysis of momentum and energy transfer in a lid-driven cavity filled with a porous medium, Int. J. Heat Mass Transfer, vol. 43(2003), pp. 3513-3527.
- [15] M. JahirulHaqueMunshi, M. A. Alim, Effect of Hydromagnetic Mixed Convection Double Lid Driven Square Cavity with Inside Elliptic Heated Block, Journal of Scientific Research, vol. 9(2016), no. 1, pp. 1- 11.
- [16] M. JahirulHaqueMunshi, M. A. Alim, M. Ali, M. ShadulAlam, “A Numerical Study of Mixed Convection in Square Lid-Driven with Internal Elliptic Body and Constant Flux Heat Source on the Bottom Wall”. Journal of Scientific Research, vol. 9(2017), no. 2, pp. 145-158.